Single-Stage Transmit Beamforming Design for MIMO Radar

Mojtaba Soltanalian*[a], Heng Hu[b], and Petre Stoica[a]

[a] *Dept. of Information Technology, Uppsala University, Uppsala, Sweden*
[b] *School of Electronic Engineering and Optoelectronics Techniques, Nanjing University of Science and Technology, Jiangsu 210094, China*
** Please address all the correspondence to Mojtaba Soltanalian, Phone: (+46) 18-471-3168; Fax: (+46) 18-511925; Email: mojtaba.soltanalian@it.uu.se*

Abstract

MIMO radar beamforming algorithms usually consist of a signal covariance matrix synthesis stage, followed by signal synthesis to fit the obtained covariance matrix. In this paper, we propose a radar beamforming algorithm (called Beam-Shape) that performs a single-stage radar transmit signal design; i.e. no prior covariance matrix synthesis is required. Beam-Shape's theoretical as well as computational characteristics, include: (i) the possibility of considering signal structures such as low-rank, discrete-phase or low-PAR, and (ii) the significantly reduced computational burden for beampattern matching scenarios with large grid size. The effectiveness of the proposed algorithm is illustrated through numerical examples.

Keywords: Beamforming, multi-input multi-output (MIMO) radar, peak-to-average-power ratio (PAR), signal design

1. Introduction

A key problem in the radar literature is the transmit signal design for matching a desired beampattern. In contrast to conventional phased-array radar, multiple-input multiple-output (MIMO) radar uses its antennas to transmit independent waveforms, and thus provides extra degrees of freedom (DOF) [1][2]. As a result, MIMO radars can achieve beampatterns which might be impossible for phased-arrays [3][4]. The MIMO radar transmit beampattern design approaches in the literature require two stages in general (see, e.g. [3]-[12]). The first stage consists of the design of the transmit covariance matrix $\boldsymbol{R}$. The design of $\boldsymbol{R}$ can be typically performed using convex optimization tools. Next, the transmit signals (under practical constraints) are designed in order to fit the obtained covariance matrix.

In this paper, we present a novel approach (which we call *Beam-Shape*) for "shaping" the transmit beam of MIMO radar via a single-stage transmit signal design. We consider the transmit beamspace processing (TBP) scheme [15] for system modeling (see Section 2 for details). Due to different practical (or computational) demands, two optimization problems are considered for both TBP weight matrix design as well as a direct design of the transmit signal. In comparison to the two-stage framework of beamforming approaches in the literature:

- Beam-Shape is able to directly consider in its formulation the matrix rank or signal constraints (such as low peak-to-average-power ratio (PAR), or discrete-phase); an advantage which generally is not shared with the covariance matrix design. As a result, the matching optimization problem will produce optimized solutions considering all the constraints of the original problem at once, and may thus avoid the optimality losses imposed by a further signal synthesis stage. See Section 4 for some numerical illustrations.

- In beamforming scenarios with large grid size, Beam-Shape appears to have a significantly smaller computational burden compared to the two-stage framework. See the related discussions in Sections 3 and 4.

Notation: We use bold lowercase letters for vectors and bold uppercase letters for matrices. $(\cdot)^T$, $(\cdot)^*$ and $(\cdot)^H$ denote the vector/matrix transpose, the complex conjugate, and the Hermitian transpose, respectively. $\mathbf{1}$ and $\mathbf{0}$ are the all-one and all-zero vectors/matrices. The symbol $\odot$ stands for the Hadamard (element-wise) product of matrices. $\|\boldsymbol{x}\|_n$ or the l_n-norm of the vector $\boldsymbol{x}$ is defined as $(\sum_k |\boldsymbol{x}(k)|^n)^{\frac{1}{n}}$ where $\{\boldsymbol{x}(k)\}$ are the entries of $\boldsymbol{x}$. The Frobenius norm of a matrix $\boldsymbol{X}$ (denoted by $\|\boldsymbol{X}\|_F$) with entries $\{\boldsymbol{X}(k,l)\}$ is equal to $\left(\sum_{k,l} |\boldsymbol{X}(k,l)|^2\right)^{\frac{1}{2}}$. We use $\Re(\boldsymbol{X})$ to denote the matrix obtained by collecting the real parts of the entries of $\boldsymbol{X}$. Finally, $\mathcal{Q}_p(\boldsymbol{X})$ yields the closest *p-ary phase matrix* with entries from the set $\{2k\pi/p : k = 0, 1, \cdots, p-1\}$, in an element-wise sense, to an argument *phase matrix* $\boldsymbol{X}$.

2. Problem Formulation

Consider a MIMO radar system with M antennas and let $\{\theta_l\}_{l=1}^{L}$ denote a fine grid of the angular sector of interest. Under the assumption that the transmitted probing signals are narrow-band and the propagation is non-dispersive, the steering vector of the transmit array (at location θ_l) can be written as

$$\boldsymbol{a}(\theta_l) = \left(e^{j2\pi f_0 \tau_1(\theta_l)}, e^{j2\pi f_0 \tau_2(\theta_l)}, \ldots, e^{j2\pi f_0 \tau_M(\theta_l)}\right)^T, \tag{1}$$

where f_0 denotes the carrier frequency of the radar, and $\tau_m(\theta_l)$ is the time needed by the transmitted signal of the m^{th} antenna to arrive at the target location θ_l.

In lieu of transmitting M partially correlated waveforms, the TBP technique employs K orthogonal waveforms that are linearly mixed at the transmit array via a weighting matrix $\boldsymbol{W} \in \mathbb{C}^{M \times K}$. The number of orthogonal waveforms K can be determined by counting the number of *significant* eigenvalues of the matrix [15]:

$$\boldsymbol{A} = \sum_{l=1}^{L} \boldsymbol{a}(\theta_l)\boldsymbol{a}^H(\theta_l). \tag{2}$$

The parameter K can be chosen such that the sum of the K dominant eigenvalues of $\boldsymbol{A}$ exceeds a given percentage of the total sum of eigenvalues [15]. Note that *usually* $K \ll M$ *(especially when* M *is large)* [15][18]. Let $\boldsymbol{\Phi}$ be the matrix containing K orthonormal TBP waveforms, viz.

$$\boldsymbol{\Phi} = (\boldsymbol{\varphi}_1, \boldsymbol{\varphi}_2, \ldots, \boldsymbol{\varphi}_K)^T \in \mathbb{C}^{K \times N}, \quad K \leq M \tag{3}$$

where $\boldsymbol{\varphi}_k \in \mathbb{C}^{N\times 1}$ denotes the k^{th} waveform (or sequence). The transmit signal matrix can then be written as $\boldsymbol{S} = \boldsymbol{W}\boldsymbol{\Phi} \in \mathbb{C}^{M\times N}$, and the transmit beampattern becomes

$$\begin{aligned} P(\theta_l) &= \|\boldsymbol{S}^H \boldsymbol{a}(\theta_l)\|_2^2 \\ &= \boldsymbol{a}^H(\theta_l)\boldsymbol{W}\boldsymbol{\Phi}\boldsymbol{\Phi}^{\boldsymbol{H}}\boldsymbol{W}^{\boldsymbol{H}}\boldsymbol{a}(\theta_l) \\ &= \boldsymbol{a}^H(\theta_l)\boldsymbol{W}\boldsymbol{W}^H\boldsymbol{a}(\theta_l) \\ &= \|\boldsymbol{W}^H\boldsymbol{a}(\theta_l)\|_2^2. \end{aligned} \tag{4}$$

Eq. (4) sheds light on two different perspectives for radar beampattern design. Observe that matching a desired beampattern may be accomplished by considering $\boldsymbol{W}$ as the design variable. Doing so, one can control the rank (K) of the covariance matrix $\boldsymbol{R} = \boldsymbol{S}\boldsymbol{S}^{\boldsymbol{H}} = \boldsymbol{W}\boldsymbol{W}^{\boldsymbol{H}}$ by fixing the dimensions of $\boldsymbol{W} \in \mathbb{C}^{M\times K}$. This idea becomes of particular interest for the phased-array radar formulation with $K = 1$. Note that considering the optimization problem with respect to $\boldsymbol{W}$ for small K may significantly reduce the computational costs. On the other hand, imposing practical signal constraints (such as discrete-phase or low PAR) while considering $\boldsymbol{W}$ as the design variable appears to be difficult. In such cases, one can resort to a direct beampattern matching by choosing $\boldsymbol{S}$ as the design variable.

In light of the above discussion, we consider beampattern matching problem formulations for designing either $\boldsymbol{W}$ or $\boldsymbol{S}$ as follows. Let $P_d(\theta_l)$ denote the desired beampattern. According to the last equality in (4), $P_d(\theta_l)$ can be synthesized exactly if and only if there exist a unit-norm vector $\boldsymbol{p}(\theta_l)$ such that

$$\boldsymbol{W}^H\boldsymbol{a}(\theta_l) = \sqrt{P_d(\theta_l)}\boldsymbol{p}(\theta_l). \tag{5}$$

Therefore, by considering $\{\boldsymbol{p}(\theta_l)\}_l$ as auxiliary design variables, the beampattern matching via weight matrix design can be dealt with conveniently via the optimization problem:

$$\min_{\boldsymbol{W},\alpha,\{\boldsymbol{p}(\theta_l)\}} \quad \sum_{l=1}^{L} \left\| \boldsymbol{W}^H \boldsymbol{a}(\theta_l) - \alpha\sqrt{P_d(\theta_l)}\boldsymbol{p}(\theta_l) \right\|_2^2 \tag{6}$$

$$\text{s.t.} \quad (\boldsymbol{W} \odot \boldsymbol{W}^*)\mathbf{1} = \tfrac{E}{M}\mathbf{1}, \tag{7}$$

$$\|\boldsymbol{p}(\theta_l)\|_2 = 1, \ \forall\, l, \tag{8}$$

where (7) is the transmission energy constraint at each transmitter with E being the total energy, and α is a scalar accounting for the energy difference between the desired beampattern and the transmitted beam. Similarly, the beampattern matching problem with $\boldsymbol{S}$ as the design variable can be formulated as

$$\min_{\boldsymbol{S},\alpha,\{\boldsymbol{p}(\theta_l)\}} \quad \sum_{l=1}^{L} \left\| \boldsymbol{S}^H \boldsymbol{a}(\theta_l) - \alpha\sqrt{P_d(\theta_l)}\boldsymbol{p}(\theta_l) \right\|_2^2 \tag{9}$$

$$\text{s.t.} \quad (\boldsymbol{S} \odot \boldsymbol{S}^*)\mathbf{1} = \tfrac{E}{M}\mathbf{1}, \tag{10}$$

$$\|\boldsymbol{p}(\theta_l)\|_2 = 1, \ \forall\, l, \tag{11}$$

$$\boldsymbol{S} \in \Psi, \tag{12}$$

where Ψ is the desired set of transmit signals. The above beampattern matching formulations pave the way for an algorithm (which we call Beam-Shape) that can perform a direct matching of the beampattern with respect to the weight matrix $\boldsymbol{W}$ or the signal $\boldsymbol{S}$, without requiring an intermediate synthesis of the covariance matrix.

3. Beam-Shape

We begin by considering the beampattern matching formulation in (6). For fixed $\boldsymbol{W}$ and α, the minimizer $\boldsymbol{p}(\theta_l)$ of (6) is given by

$$\boldsymbol{p}(\theta_l) = \frac{\boldsymbol{W}^H \boldsymbol{a}(\theta_l)}{\|\boldsymbol{W}^H \boldsymbol{a}(\theta_l)\|_2}. \tag{13}$$

Let $P \triangleq \sum_{l=1}^{L} P_d(\theta_l)$. For fixed $\boldsymbol{W}$ and $\{\boldsymbol{p}(\theta_l)\}$ the minimizer α of (6) can be obtained as

$$\alpha = \Re\left\{ \left(\sum_{l=1}^{L} \sqrt{P_d(\theta_l)}\boldsymbol{p}^H(\theta_l)\boldsymbol{W}^H \boldsymbol{a}(\theta_l) \right) / P \right\}. \tag{14}$$

Using (13), the expression for α can be further simplified as

$$\alpha = \left(\sum_{l=1}^{L} \sqrt{P_d(\theta_l)} \left\| \boldsymbol{W}^H \boldsymbol{a}(\theta_l) \right\|_2 \right) / P. \tag{15}$$

Now assume that $\{\boldsymbol{p}(\theta_l)\}$ and α are fixed. Note that

$$\begin{aligned} Q(\boldsymbol{W}) &= \sum_{l=1}^{L} \|\boldsymbol{W}^H \boldsymbol{a}(\theta_l) - \alpha \sqrt{P_d(\theta_l)} \boldsymbol{p}(\theta_l)\|_2^2 \\ &= \mathrm{tr}(\boldsymbol{W}\boldsymbol{W}^H \boldsymbol{A}) - 2\Re\{\mathrm{tr}(\boldsymbol{W}\boldsymbol{B})\} + P\alpha^2 \end{aligned} \tag{16}$$

where $\boldsymbol{A}$ is as defined in (2), and

$$\boldsymbol{B} = \sum_{l=1}^{L} \alpha \sqrt{P_d(\theta_l)} \boldsymbol{p}(\theta_l) \boldsymbol{a}^H(\theta_l). \tag{17}$$

By dropping the constant part in $Q(\boldsymbol{W})$, we have

$$\begin{aligned} \widetilde{Q}(\boldsymbol{W}) &= \mathrm{tr}(\boldsymbol{W}\boldsymbol{W}^H \boldsymbol{A}) - 2\Re\left\{\mathrm{tr}(\boldsymbol{W}\boldsymbol{B})\right\} \qquad (18) \\ &= \mathrm{tr}\left(\begin{pmatrix} \boldsymbol{W} \\ \boldsymbol{I} \end{pmatrix}^H \underbrace{\begin{pmatrix} \boldsymbol{A} & -\boldsymbol{B}^H \\ -\boldsymbol{B} & \boldsymbol{0} \end{pmatrix}}_{\triangleq \boldsymbol{C}} \underbrace{\begin{pmatrix} \boldsymbol{W} \\ \boldsymbol{I} \end{pmatrix}}_{\triangleq \widetilde{\boldsymbol{W}}} \right). \end{aligned}$$

Therefore, the minimization of (6) with respect to $\boldsymbol{W}$ is equivalent to

$$\begin{aligned} \min_{\boldsymbol{W}} \quad & \mathrm{tr}\left(\widetilde{\boldsymbol{W}}^H \boldsymbol{C} \widetilde{\boldsymbol{W}} \right) && (19) \\ \text{s.t.} \quad & (\boldsymbol{W} \odot \boldsymbol{W}^*)\boldsymbol{1} = \tfrac{E}{M}\boldsymbol{1}, && (20) \\ & \widetilde{\boldsymbol{W}} = \left(\boldsymbol{W}^T \ \boldsymbol{I} \right)^T. && (21) \end{aligned}$$

As a result of the energy constraint in (20), $\widetilde{\boldsymbol{W}}$ has a fixed Frobenius norm, and hence a diagonal loading of $\boldsymbol{C}$ does not change the solution to (19). Therefore, (19) can be written in the following equivalent form:

$$\begin{aligned} \max_{\boldsymbol{W}} \quad & \mathrm{tr}\left(\widetilde{\boldsymbol{W}}^H \widetilde{\boldsymbol{C}} \widetilde{\boldsymbol{W}} \right) && (22) \\ \text{s.t.} \quad & (\boldsymbol{W} \odot \boldsymbol{W}^*)\boldsymbol{1} = \tfrac{E}{M}\boldsymbol{1}, && (23) \\ & \widetilde{\boldsymbol{W}} = \left(\boldsymbol{W}^T \ \boldsymbol{I} \right)^T && (24) \end{aligned}$$

where $\widetilde{\boldsymbol{C}} = \lambda \boldsymbol{I} - \boldsymbol{C}$, with λ being larger than the maximum eigenvalue of $\boldsymbol{C}$. In particular, *an increase in the objective function of (22) leads to a decrease of the objective function in (6).* Although (22) is non-convex, a monotonically increasing sequence of the objective function in (22) may be obtained (see the Appendix for a proof) via a generalization of the *power method-like iterations* proposed in [19] and [20], namely:

$$\boldsymbol{W}^{(t+1)} = \sqrt{\frac{E}{M}}\,\eta\left(\begin{pmatrix} \boldsymbol{I}_{M\times M} \\ \boldsymbol{0} \end{pmatrix}^T \widetilde{\boldsymbol{C}}\,\widetilde{\boldsymbol{W}}^{(t)}\right) \tag{25}$$

where the iterations may be initialized with the latest approximation of $\boldsymbol{W}$ (used as $\boldsymbol{W}^{(0)}$), t denotes the internal iteration number, and $\eta(\cdot)$ is a row-scaling operator that makes the rows of the matrix argument have unit-norm.

Next we study the optimization problem in (9). Thanks to the similarity of the problem formulation to (6), the derivations of the minimizers $\{\boldsymbol{p}(\theta_l)\}$ and α of (9) remain the same as for (6). Moreover, the minimization of (9) with respect to the constrained $\boldsymbol{S}$ can be formulated as the following optimization problem:

$$\max_{\boldsymbol{S}} \quad \operatorname{tr}\left(\widetilde{\boldsymbol{S}}^H \widetilde{\boldsymbol{C}} \widetilde{\boldsymbol{S}}\right) \tag{26}$$

$$\text{s.t.} \quad (\boldsymbol{S} \odot \boldsymbol{S}^*)\boldsymbol{1} = \tfrac{E}{M}\boldsymbol{1}, \tag{27}$$

$$\widetilde{\boldsymbol{S}} = \left(\boldsymbol{S}^T \boldsymbol{I}\right)^T, \ \boldsymbol{S} \in \Psi \tag{28}$$

with $\widetilde{\boldsymbol{C}}$ being the same as in (22). An increasing sequence of the objective function in (26) can be obtained via power method-like iterations that exploit the following nearest-matrix problem (see the Appendix for a sketched proof):

$$\min_{\boldsymbol{S}^{(t+1)}} \quad \left\| \boldsymbol{S}^{(t+1)} - \begin{pmatrix} \boldsymbol{I}_{M\times M} \\ \boldsymbol{0} \end{pmatrix}^T \widetilde{\boldsymbol{C}}\,\widetilde{\boldsymbol{S}}^{(t)} \right\|_F \tag{29}$$

$$\text{s.t.} \quad (\boldsymbol{S}^{(t+1)} \odot \boldsymbol{S}^{*\,(t+1)})\boldsymbol{1} = \tfrac{E}{M}\boldsymbol{1}, \ \ \boldsymbol{S}^{(t+1)} \in \Psi. \tag{30}$$

Obtaining the solution to (29) for some constraint sets Ψ such as real-valued, unimodular, or p-ary matrices is straightforward, viz.

$$\boldsymbol{S}^{(t+1)} = \begin{cases} \sqrt{\frac{E}{M}}\ \eta\left(\Re\left\{\widehat{\boldsymbol{S}}^{(t)}\right\}\right), & \Psi = \text{real-values matrices}, \\ e^{j\arg\left(\widehat{\boldsymbol{S}}^{(t)}\right)}, & \Psi = \text{unimodular matrices}, \\ e^{j\mathcal{Q}_p\left(\arg\left(\widehat{\boldsymbol{S}}^{(t)}\right)\right)}, & \Psi = p\text{-ary matrices}, \end{cases} \tag{31}$$

where

$$\widehat{\boldsymbol{S}}^{(t)} = \begin{pmatrix} \boldsymbol{I}_{M\times M} \\ \boldsymbol{0} \end{pmatrix}^T \widetilde{\boldsymbol{C}}\,\widetilde{\boldsymbol{S}}^{(t)}. \tag{32}$$

Furthermore, the case of PAR-constrained $\boldsymbol{S}$ can be handled efficiently via a recursive algorithm devised in [21].

Finally, the Beam-Shape algorithm for beampattern matching via designing the weight matrix $\boldsymbol{W}$ or the transmit signal $\boldsymbol{S}$ is summarized in Table 1.

Remark: A brief comparison of the computational complexity of the Beam-Shape algorithm and the two-stage beamforming approaches in the literature is as follows. The design of the covariance matrix $\boldsymbol{R} \in \mathbb{C}^{M\times M}$ for the two-stage framework can be done using a semi-definite program (SDP) representation with $\mathcal{O}(L)$ constraints. The corresponding SDP may be solved with $\mathcal{O}(\max\{M,L\}^4 M^{1/2}\log(1/\epsilon))$ complexity, where $\epsilon > 0$ denotes the solution accuracy [22]. Using the formulation in [4], the design of $\boldsymbol{W}$ or $\boldsymbol{S}$ (for fitting the given covariance matrix) leads to an iterative approach with an iteration complexity of $\mathcal{O}(M^2K + KM^2 + K^3)$, or $\mathcal{O}(M^2N + NM^2 + N^3)$, respectively. On the other hand, Beam-Shape is an iterative method with an iteration complexity of $\mathcal{O}(M(L+KH)(M+K))$ for designing $\boldsymbol{W}$, and $\mathcal{O}(M(L+NH)(M+N))$ for designing $\boldsymbol{S}$; where H denotes the number of required internal iterations of the power method-like methods discussed in (25) or (29). The above results suggest that *Beam-Shape may be more computationally efficient when the grid size (L) grows large.* The next section provides numerical examples for further computational efficiency comparison between the two approaches. ■

Table 1: The Beam-Shape algorithm for MIMO radar beamforming

Step 0: Calculate the matrix $\boldsymbol{A}$ using (2). Choose random α and $\{\boldsymbol{p}(\theta_l)\}$ and initialize the matrix $\boldsymbol{B}$ using (17).
Step 1: Use the power method-like iterations in (25) (until convergence) to obtain $\boldsymbol{W}$, or (29) to obtain $\boldsymbol{S}$.
Step 2: Update $\{\boldsymbol{p}(\theta_l)\}$, α, and $\boldsymbol{B}$ using (13), (15), and (17), respectively.
Step 3: Repeat steps 1 and 2 until a stop criterion is satisfied, e.g. $\|\boldsymbol{W}^{(v+1)} - \boldsymbol{W}^{(v)}\|_F < \varepsilon$ for some given $\varepsilon > 0$, where v denotes the total iteration number.

4. Numerical Examples with Discussions

In this section, we provide several numerical examples to show the potential of Beam-Shape in applications. Consider a MIMO radar with a uniform linear array (ULA) comprising $M = 32$ antennas with half-wavelength spacing between adjacent antennas. The total transmit power is set to $E = MN$. The angular pattern covers $[-90°, 90°]$ with a mesh grid size of $1°$ and the desired beampattern is given by

$$P_d(\theta) = \begin{cases} 1, \ \theta \in [\widehat{\theta}_k - \Delta, \widehat{\theta}_k + \Delta] \\ 0, \ \text{otherwise} \end{cases} \tag{33}$$

where $\widehat{\theta}_k$ denotes the direction of a target of interest and 2Δ is the chosen beamwidth for each target. In the following examples, we assume 3 targets located at $\widehat{\theta}_1 = -45°$, $\widehat{\theta}_2 = 0°$ and $\widehat{\theta}_3 = 45°$ with a beamwidth of $24°$ ($\Delta = 12°$). The results are compared with those obtained via the covariance matrix synthesis-based (CMS) approach proposed in [3] and [4]. For the sake of a fair comparison, we define the mean square error (MSE) of a beampattern matching as

$$\text{MSE} \triangleq \sum_{l=1}^{L} \left| \boldsymbol{a}^H(\theta_l) \boldsymbol{R}\, \boldsymbol{a}(\theta_l) - P_d(\theta_l) \right|^2 \tag{34}$$

which is the typical optimality criterion for the covariance matrix synthesis in the literature (including the CMS in [3] and [4]).

We begin with the design of the weight matrix $\boldsymbol{W}$ using the formulation in (6). In particular, we consider $K = M$ corresponding to a general MIMO radar,

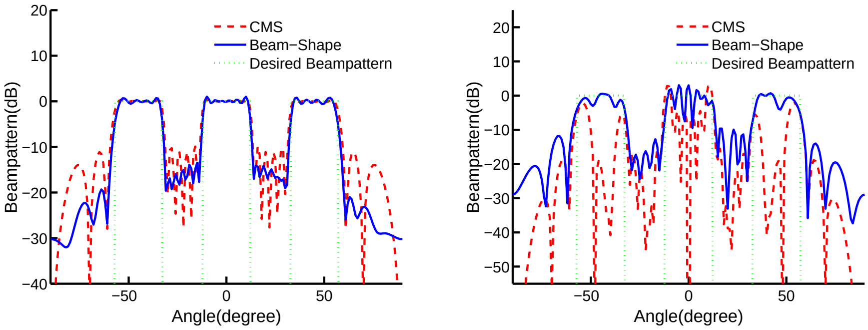

(a) (b)

Figure 1: Comparison of radar beampattern matchings obtained by CMS and Beam-Shape using the weight matrix $\boldsymbol{W}$ as the design variable: (a) $K = M$ corresponding to a general MIMO radar, and (b) $K = 1$ which corresponds to a phased-array.

and $K = 1$ which corresponds to a phased-array. The results are shown in Fig. 1. For $K = M$, The MSE values obtained by Beam-Shape and CMS are 1.79 and 1.24, respectively. Note that a smaller MSE value was expected for CMS in this case, as CMS obtains $\boldsymbol{R}$ (or equivalently $\boldsymbol{W}$) by globally minimizing the MSE in (34). On the other hand, in the phased-array example (Fig. 1(b)), Beam-Shape yields an MSE value of 3.72, whereas the MSE value obtained by CMS is 7.21. Such a behavior was also expected due to the embedded rank constraint when designing $\boldsymbol{W}$ by Beam-Shape, while CMS appears to face a considerable loss during the synthesis of the rank-constrained $\boldsymbol{W}$.

Next we design the transmit signal $\boldsymbol{S}$ using the formulation in (9). In this example, $\boldsymbol{S}$ is constrained to be unimodular (i.e. $|\boldsymbol{S}(k,l)| = 1$), which corresponds to a unit PAR. Fig. 2 compares the performances of Beam-Shape and CMS for two different lengths of the transmit sequences, namely $N = 8$ (Fig. 2(a)) and $N = 128$ (Fig. 2(b)). In the case of $N = 8$, Beam-Shape obtains an MSE value of 1.80 while the MSE value obtained by CMS is 2.73. For $N = 128$, the MSE values obtained by Beam-Shape and CMS are 1.74 and 1.28, respectively. Given the fact that $M = 32$, the case of $N = 128$ provides a large number of DOFs for CMS when fitting $\boldsymbol{S}\boldsymbol{S}^H$ to the obtained $\boldsymbol{R}$ in the covariance matrix

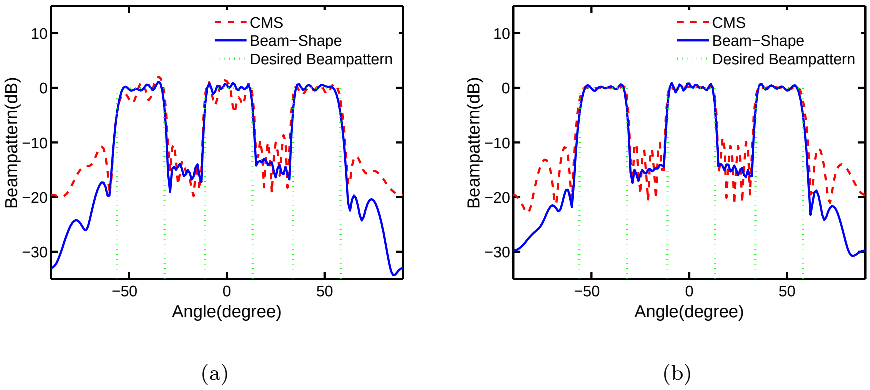

Figure 2: Comparison of MIMO radar beampattern matchings obtained by CMS and Beam-Shape using the signal matrix $\boldsymbol{S}$ as the design variable: (a) $N = 8$, (b) $N = 128$.

synthesis stage, whereas for $N = 8$ the number of DOFs is rather limited.

Finally, it can be interesting to examine the performance of Beam-Shape in scenarios with large grid size L. To this end, we compare the computation times of Beam-Shape and CMS for different L, using the same problem setup for designing $\boldsymbol{S}$ (as the above example) but for $N = M = 32$. According to Fig. 3, the overall CPU time of CMS is growing rapidly as L increases, which implies that CMS can hardly be used for beamforming design with large grid sizes (e.g. $L \gtrsim 10^3$). In contrast, Beam-Shape runs well for large L, even for $L \sim 10^6$ on a standard PC. The results leading to Fig. 3 were obtained by averaging the computation times for 100 experiments (with different random initializations) using a PC with Intel Core i5 CPU 750 @2.67GHz, and 8GB memory.

Appendix A. Power Method-Like Iterations Monotonically Increase the Objective Functions in (22) and (26)

In the following, we study the power method-like iterations for designing $\boldsymbol{W}$ in (22). The extension of the results to the design of $\boldsymbol{S}$ in (26) is straightforward. For fixed $\boldsymbol{W}^{(t)}$, observe that the update matrix $\boldsymbol{W}^{(t+1)}$ is the minimizer of the

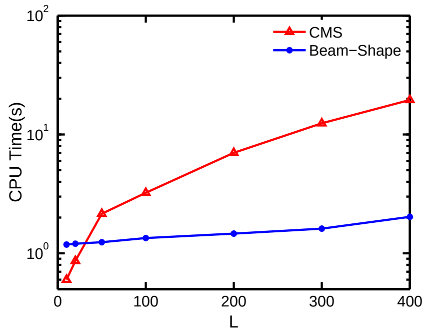

Figure 3: Comparison of computation times for Beam-Shape and CMS with different grid sizes L.

criterion

$$\left\| \widetilde{\boldsymbol{W}}^{(t+1)} - \widetilde{\boldsymbol{C}}\widetilde{\boldsymbol{W}}^{(t)} \right\|_2^2 = \text{const} - 2\Re\left\{ \text{tr}\left(\widetilde{\boldsymbol{W}}^{(t+1)\,H} \widetilde{\boldsymbol{C}}\widetilde{\boldsymbol{W}}^{(t)} \right) \right\} \tag{A.1}$$

or, equivalently, the maximizer of the criterion

$$\Re\left\{ \text{tr}\left(\widetilde{\boldsymbol{W}}^{(t+1)\,H} \widetilde{\boldsymbol{C}}\widetilde{\boldsymbol{W}}^{(t)} \right) \right\} \tag{A.2}$$

in the search space satisfying the given fixed-norm constraint on the rows of $\boldsymbol{W}$ (for $\boldsymbol{S}$, one should also consider the constraint set Ψ). Therefore, for the optimizer $\widetilde{\boldsymbol{W}}^{(t+1)}$ of (22) we must have

$$\Re\left\{ \text{tr}\left(\widetilde{\boldsymbol{W}}^{(t+1)\,H} \widetilde{\boldsymbol{C}}\widetilde{\boldsymbol{W}}^{(t)} \right) \right\} \geq \text{tr}\left(\widetilde{\boldsymbol{W}}^{(t)\,H} \widetilde{\boldsymbol{C}}\widetilde{\boldsymbol{W}}^{(t)} \right). \tag{A.3}$$

Moreover, as $\widetilde{\boldsymbol{C}}$ is positive-definite:

$$\text{tr}\left(\left(\widetilde{\boldsymbol{W}}^{(t+1)} - \widetilde{\boldsymbol{W}}^{(t)} \right)^H \widetilde{\boldsymbol{C}} \left(\widetilde{\boldsymbol{W}}^{(t+1)} - \widetilde{\boldsymbol{W}}^{(t)} \right) \right) \geq 0 \tag{A.4}$$

which along with (A.3) implies

$$\text{tr}\left(\widetilde{\boldsymbol{W}}^{(t+1)\,H} \widetilde{\boldsymbol{C}}\widetilde{\boldsymbol{W}}^{(t+1)} \right) \geq \text{tr}\left(\widetilde{\boldsymbol{W}}^{(t)\,H} \widetilde{\boldsymbol{C}}\widetilde{\boldsymbol{W}}^{(t)} \right), \tag{A.5}$$

and hence, a monotonic increase of the objective function in (22).

Acknowledgement

This work was supported in part by the European Research Council (ERC) under Grant #228044 and the Swedish Research Council.

References

[1] J. Li, P. Stoica, MIMO radar with colocated antennas, IEEE Signal Processing Magazine 24 (5) (2007) 106–114.

[2] A. M. Haimovich, R. S. Blum, L. J. Cimini, MIMO radar with widely separated antennas, IEEE Signal Processing Magazine 25 (1) (2008) 116–129.

[3] P. Stoica, J. Li, X. Yao, On probing signal design for MIMO radar, IEEE Transactions on Signal Processing 55 (8) (2007) 4151–4161.

[4] P. Stoica, J. Li, X. Zhu, Waveform synthesis for diversity-based transmit beampattern design, IEEE Transactions on Signal Processing 56 (6) (2008) 2593–2598.

[5] P. Gong, Z. Shao, G. Tu, Q. Chen, Transmit beampattern design based on convex optimization for MIMO radar systems, Signal Processing 94 (2014) 195–201.

[6] T. Aittomaki, V. Koivunen, Signal covariance matrix optimization for transmit beamforming in MIMO radars, in: Asilomar Conference on Signals, Systems and Computers, 2007, pp. 182–186.

[7] T. Aittomaki, V. Koivunen, Low-complexity method for transmit beamforming in MIMO radars, in: IEEE International Conference on Acoustics, Speech and Signal Processing (ICASSP), Vol. 2, 2007, pp. 305–308.

[8] D. R. Fuhrmann, G. San Antonio, Transmit beamforming for MIMO radar systems using signal cross-correlation, IEEE Transactions on Aerospace and Electronic Systems 44 (1) (2008) 171–186.

[9] G. Hua, S. Abeysekera, MIMO radar transmit beampattern design with ripple and transition band control, IEEE Transactions on Signal Processing 61 (11) (2013) 2963–2974. doi:10.1109/TSP.2013.2252173.

[10] K. Shadi, F. Behnia, MIMO radar beamforming using orthogonal decomposition of correlation matrix, Circuits, Systems, and Signal Processing (2013) 1–19.

[11] S. Ahmed, J. S. Thompson, Y. R. Petillot, B. Mulgrew, Unconstrained synthesis of covariance matrix for MIMO radar transmit beampattern, IEEE Transactions on Signal Processing 59 (8) (2011) 3837–3849.

[12] H. Xu, J. Wang, J. Yuan, X. Shan, MIMO radar transmit beampattern synthesis via minimizing sidelobe level, Progress In Electromagnetics Research B 53 (2013) 355–371.

[13] H. He, J. Li, P. Stoica, Waveform design for active sensing systems: a computational approach, Cambridge University Press, 2012.

[14] A. Khabbazibasmenj, S. A. Vorobyov, A. Hassanien, Robust adaptive beamforming via estimating steering vector based on semidefinite relaxation, in: Conference Record of the Forty Fourth Asilomar Conference on Signals, Systems and Computers (ASILOMAR), IEEE, 2010, pp. 1102–1106.

[15] A. Hassanien, S. A. Vorobyov, Transmit energy focusing for DOA estimation in MIMO radar with colocated antennas, IEEE Transactions on Signal Processing 59 (6) (2011) 2669–2682.

[16] C. Xiang, D.-Z. Feng, H. Lv, J. He, Y. Cao, Robust adaptive beamforming for MIMO radar, Signal Processing 90 (12) (2010) 3185–3196.

[17] M. Soltanalian, M. M. Naghsh, P. Stoica, A fast algorithm for designing complementary sets of sequences, Signal Processing 93 (7) (2013) 2096–2102.

[18] A. Hassanien, M. W. Morency, A. Khabbazibasmenj, S. A. Vorobyov, J.-Y. Park, S.-J. Kim, Two-dimensional transmit beamforming for MIMO radar with sparse symmetric arrays, in: IEEE Radar Conference, 2013.

[19] M. Soltanalian, P. Stoica, Designing unimodular codes via quadratic optimization, IEEE Transactions on Signal Processing.

[20] M. Soltanalian, B. Tang, J. Li, P. Stoica, Joint design of the receive filter and transmit sequence for active sensing, IEEE Signal Processing Letters 20 (5) (2013) 423–426.

[21] J. A. Tropp, I. S. Dhillon, R. W. Heath, T. Strohmer, Designing structured tight frames via an alternating projection method, IEEE Transactions on Information Theory 51 (1) (2005) 188–209.

[22] Z.-q. Luo, W.-k. Ma, A.-C. So, Y. Ye, S. Zhang, Semidefinite relaxation of quadratic optimization problems, IEEE Signal Processing Magazine 27 (3) (2010) 20–34.

[23] J. Li, P. Stoica (Eds.), Robust adaptive beamforming, Wiley, New York, 2006.

[24] B. Friedlander, On transmit beamforming for MIMO radar, IEEE Transactions on Aerospace and Electronic Systems 48 (4) (2012) 3376–3388.

[25] A. Srinivas, V. Reddy, Transmit beamforming for colocated MIMO radar, in: International Conference on Signal Processing and Communications (SPCOM), IEEE, Bangalore, India, 2010, pp. 1–5.

[26] W. Rowe, M. Ström, J. Li, P. Stoica, Robust adaptive beamforming for MIMO monopulse radar, in: SPIE Defense, Security, and Sensing, International Society for Optics and Photonics, Baltimore, Maryland, USA, 2013, pp. 1–15.